Ferromagnetic versus antiferromagnetic interaction in Co-doped ZnO

Eun-Cheol Lee and K. J. Chang
Department of Physics, Korea Advanced Institute of Science and Technology, Daejeon 305-701, Korea
(Received 23 July 2003; published 19 February 2004)

Based on first-principles spin-density functional calculations, we find that Co-doped ZnO energetically favors a spin-glass-like state due to antiferromagnetic interactions between transition metal atoms, while ferromagnetic ordering is stabilized by electron doping. We find a short range nature in both antiferromagnetic and ferromagnetic interactions, and suggest that a very high doping level of Co ions is required to achieve ferromagnetism, together with a sufficient supply of electron carriers. Our results explain experimental features such as the low reproducibility of ferromagnetic samples and the very low saturation magnetization per Co ion.

DOI: 10.1103/PhysRevB.69.085205 PACS number(s): 75.50.Pp, 71.20.Nr, 75.30.Et, 75.30.Hx

Diluted magnetic semiconductors (DMSs), where transition metal atoms are introduced into the cations of the semiconducting host, have attracted much attention because of the potential use of both charge and spin of electrons for spintronic devices.[1] A promising technique is to use DMSs to inject spin-polarized carriers into nonmagnetic semiconductors. Recently, spin injection using Mn-doped III-V-based semiconductors has been successfully demonstrated; however, devices only work at low temperatures far below room temperature because of the low Curie temperature (T_c) for these materials.[2] For practical applications, it is a key issue to raise the T_c of DMSs above room temperature, and room temperature ferromagnetism has been observed for several magnetically doped materials such as ZnO, GaN, and $ZnGeP_2$.[3–5]

Among room temperature ferromagnetic semiconductors, ZnO has been of special interest because this material is optically transparent with a wide band gap of 3.3 eV and a large exciton binding energy of 60 meV.[6] Especially, in Co-doped ZnO, there have been several experiments reporting room temperature ferromagnetism.[3,7–9] However, experimental results are quite controversial; Ueda *et al.* succeeded in obtaining room temperature ferromagnetism only in a few samples showing metallic conduction with electron concentrations as high as 10^{20} cm^{-3}, while other samples exhibited a spin-glass behavior.[3] This experiment indicated that high electron carrier concentrations seem to be essential for the ferromagnetism; however, other experiments showed quite different results, observing no ferromagnetism even in samples with carrier concentrations over 10^{20} cm^{-3}.[10] The existence of ferromagnetic ordering in Co-doped ZnO was first theoretically proposed, which is attributed to the double exchange interaction between Co ions,[11] while later calculations suggested the Ruderman-Kittel-Kasuya-Yosida (RKKY) interaction as the origin of ferromagnetism.[12] As other possible origins for the ferromagnetism, the formation of CoO or Co-metal clusters was also considered.[3,13]

In this paper, we find that antiferromagnetic couplings are preferred between transition metal atoms in Co-doped ZnO, resulting in a spin-glass state, while ferromagnetic ordering is realized by electron doping, based on first-principles spin-density functional calculations. Due to the short range nature of the ferromagnetic coupling, a heavy incorporation of Co atoms is required to stabilize the ferromagnetic state. However, this process simultaneously reduces the amount of doped electrons per Co ion, weakening the ferromagnetic interaction. Our results explain the low reproducibility of ferromagnetism and very low saturation magnetization per Co atom in Co-doped samples, and provide optimum conditions for achieving the ferromagnetic state.

Our calculations are performed within the local-spin-density functional approximation using the generalized gradient correction for the exchange-correlation energy.[14] We use ultrasoft pseudopotentials for the efficient treatment of the localized orbitals of the O, Zn, and Co atoms.[15] The wave functions are expanded in plane waves up to a cutoff of 30 Ry, which ensures an energy precision of better than 1 meV per two Co atoms in comparing ferromagnetic and antiferromagnetic states. Ionic coordinates are fully optimized with the use of the conjugate gradient technique. We choose various supercells which are formed by integer multiples ($n_1\boldsymbol{a}_1$, $n_2\boldsymbol{a}_2$, and $n_3\boldsymbol{a}_3$) of the primitive lattice vectors, $\boldsymbol{a}_1$, $\boldsymbol{a}_2$, and $\boldsymbol{a}_3$, of the wurtzite structure, and thus denoted by $n_1\times n_2\times n_3$. For the summation of charge densities over the Brillouin zone, we choose a *k*-point set which is equivalent to that generated by the $8\times8\times4$ Monkhorst-Pack mesh for the $1\times1\times1$ primitive cell.[16] For charged systems, we use a jellium background that eliminates the divergence in the energy of the periodically repeated charged system.

For a Co ion occupying a cation site, we use the $2\times2\times1$ supercell to examine hybridizations between Co and O orbitals. Compared with a pure ZnO, we find that majority and minority spins have similar ZnO-derived bands, while the valence and conduction band edges of minority spins are slightly shifted by about 0.16 and 0.08 eV, respectively, due to *p*-*d* and *s*-*d* exchange splittings, as shown in Figs. 1(a) and 1(b). From the projected densities of states in Fig. 1(c), major hybridizations occur between Co *d* and O *p* orbitals, forming bonding t^b and antibonding t^a states, with nonbonding *e* states lying between the two states. For majority spins, the *e* and t^a states are located between 0 and 1.10 eV, i.e., in the band gap, while they lie in the conduction band for minority spins, with the intraionic exchange splittings of 1.4 and 2.4 eV, respectively, similar to previous calculations.[11]

To see the origin of ferromagnetism in $Zn_{1-x}Co_xO$ alloys, we first investigate magnetic interactions between Co ions, especially the interaction range and dependence on the crystal direction. We choose the $2\times2\times1$ supercell containing

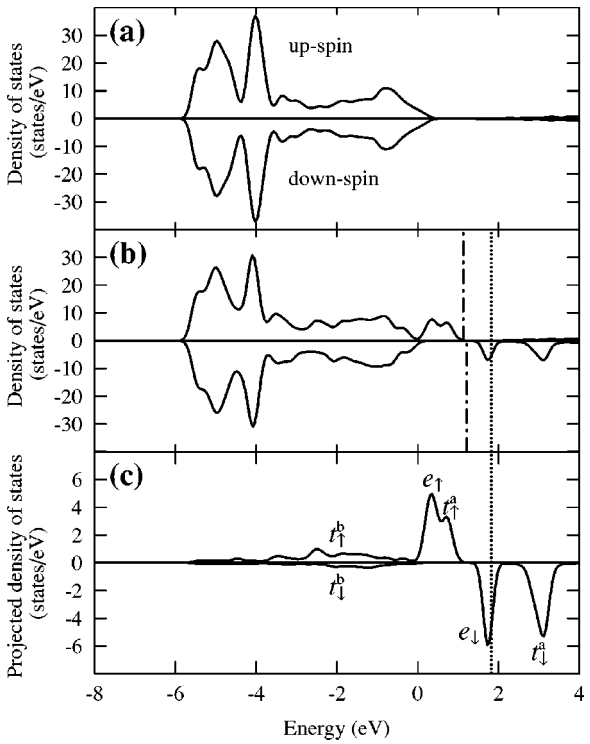

FIG. 1. (a) The total density of states for (a) pure and (b) Co-doped ZnO, and (c) Co $3d$-projected density of states for electrons with up- and down-spins in Co-doped ZnO. For Co-doped ZnO, the $2\times2\times1$ supercell is used with containing a Co atom at the Zn lattice. The dotted and dot-dashed vertical lines indicate the Fermi level and the conduction band minimum, respectively.

two Co atoms, which leads to the Co doping level of $x=0.25$. When Co atoms are aligned along the $\boldsymbol{a}_1$ direction on the hexagonal plane, the distance between nearest neighboring Co atoms is 3.28 Å, and 3.23 Å along the c axis, i.e., the $\boldsymbol{a}_3$ direction [see Figs. 2(a) and 2(b)]. When Co ions are

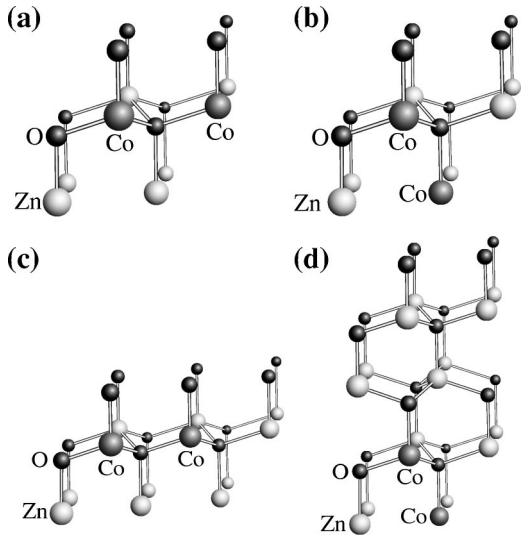

FIG. 2. Supercell geometries for Co ions continuously aligned along the (a) $\boldsymbol{a}_1$ and (b) $\boldsymbol{a}_3$ directions, and those paired along the (c) $\boldsymbol{a}_1$ and (d) $\boldsymbol{a}_3$ directions.

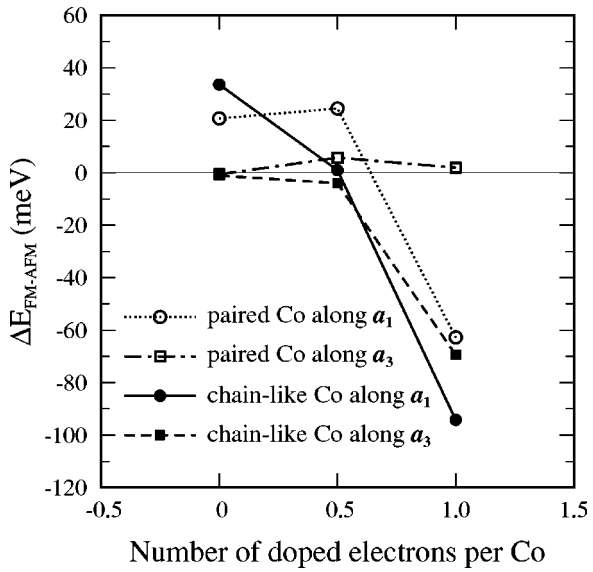

FIG. 3. The total energy differences ($\Delta E_{\text{FM-AFM}}$) between the ferromagnetic and antiferromagnetic states are plotted as a function of the amount of doped electrons for Co ions paired and continuously aligned (chain-like) along the $\boldsymbol{a}_1$ and $\boldsymbol{a}_3$ (i.e., c-axis) directions.

continuously aligned along the $\boldsymbol{a}_1$ direction, the antiferromagnetic (AFM) solution is energetically more stable by about 34 meV per Co atom than the ferromagnetic (FM) state, while the FM state is lower in energy by about 1 meV per Co atom for the alignment on the c axis, as shown in Fig. 3. The difference in the stability of magnetic states between the two alignments of Co atoms results from the hexagonal symmetry of the wurtzite structure, which affects the magnitude of superexchange interaction. The superexchange interaction arises from the coupling of magnetic d holes in half-filled t orbitals, while it vanishes for almost fully filled e orbitals. Since the bond angle between two Co-O bonds is about 109.5°, we expect finite superexchange couplings between t orbitals according to the Goodenough-Kanamori rules[17] for the antiferromagnetic state, which predicted the absence of superexchange coupling for the bond angle of 90°. Analyzing the empty $t^a_\downarrow$ states, we find that interactions between d holes via ligand p orbitals strongly depend on the alignment direction of Co atoms, causing the difference in the superexchange coupling. Along the $\boldsymbol{a}_1$ axis, the two Co ions, Co_I and Co_II in the supercell (see Fig. 4), are located in the same crystal fields, and thus their d orbitals effectively interact with a mediating O $2p$ orbital. Since the interacting lobes of Co-d and O-p orbitals form an angle of about 35.3°, both $dp\pi$ and $dp\sigma$ interactions exist between the O and two neighboring Co atoms. On the other hand, for Co ions along the c axis, weak $dp\pi$-type interactions exist between the O and one (Co_I) of the two neighboring Co atoms, significantly reducing the magnitude of the electron (or hole) transfer matrix element (b), while the d orbital of the other Co atom (Co_II) strongly interact with the O p orbital via the $dp\sigma$-type coupling. Thus, the AFM coupling is much weakened for Co ions aligned along the c axis, since the superexchange interaction is proportional to b^2/U,[18] where U is the repulsive Coulomb interaction energy.

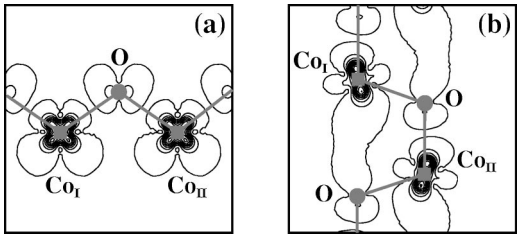

FIG. 4. The charge density contours are plotted for the $t_{\downarrow}^{a}$ orbitals which predominantly contribute to the antiferromagnetic superexchange interaction, with a contour spacing of 0.03 a.u. In (a) and (b), Co ions are aligned along the $\boldsymbol{a}_1$- and c-axis directions, respectively.

We also find similar results for the superexchange interaction, with use of larger $3\times2\times1$ and $2\times2\times2$ supercells containing the same number of Co ions, where Co ions are in fact paired along the $\boldsymbol{a}_1$- and c-axis directions, respectively, with pair-pair distances of 9.84 and 10.5 Å [see Figs. 2(c) and 2(d)]. For Co pairs along the $\boldsymbol{a}_1$ axis, the AFM state is still energetically more favorable by 21 meV per Co atom, but the energy difference between the antiferromagnetic and ferromagnetic states is decreased by 13 meV/Co due to reduced hybridizations between the Co and O atoms. For Co pairs along the c axis, the stability of the AFM state is not affected. To find the range of interactions between Co atoms, we test various geometries for a Co pair in the supercell, increasing the Co-Co distance from 3.28 (or 3.23) to 4.61, 5.25, and 6.56 Å. The type of adopted supercells and the coordinates of Co atoms for each case are listed in Table I. Although the supercell size may not be large enough to examine pure magnetic interactions between two isolated Co ions, the order of magnitude of magnetic couplings can be accurately estimated. For all cases, we find that the total energy differences between the FM and AFM states are less than 3 meV per Co atom, almost independent of the Co-Co distance. These results indicate that couplings between two Co ions are negligible for distances larger than 4.6 Å, suggesting that the range of magnetic interactions is rather short. For $Ge_{1-x}Mn_x$, recent calculations showed that exchange interactions greatly fluctuate at similar distances between metal ions, obeying the RKKY formula.[19] For Co-doped ZnO, however, the magnetic properties seem to be predominantly determined by Co-Co interactions over a small region of about 3 Å, i.e., the nearest-neighbor distance of Co ions. We point out that although the alignment of Co atoms along the c-axis favors the FM state mainly due to weakening of AFM superexchange interactions, the FM state is unlikely to be stabilized because of the very small energy difference between the FM and AFM states. Thus, contrary to previous calculations,[11] our results suggest that Co-doped ZnO energetically prefers the spin-glass-like state to the ferromagnetic ordering.

TABLE I. The total energies (E_{FM} in units of meV per Co atom) of the ferromagnetic state relative to the antiferromagnetic configuration are compared for various Co-Co distances (d). For each supercell, the coordinates of Co_{II} are given in terms of the primitive lattice vectors in the wurtzite structure (Ref. 23), while Co_I is positioned at the origin. Here N_e denotes the number of doped electrons per Co atom.

	$d=4.61$ Å	$d=5.26$ Å	$d=6.56$ Å
Supercell	$2\times2\times2$	$2\times1\times2$	$4\times1\times1$
Coordinate of Co_{II}	(2/3,2/3,1/2)	(0,0,1)	(2,0,0)
E_{FM} for $N_e=0$	0.1	1.7	2.8
E_{FM} for $N_e=0.5$	1.0	2.5	1.4
E_{FM} for $N_e=1.0$	−4.1	3.8	0.4

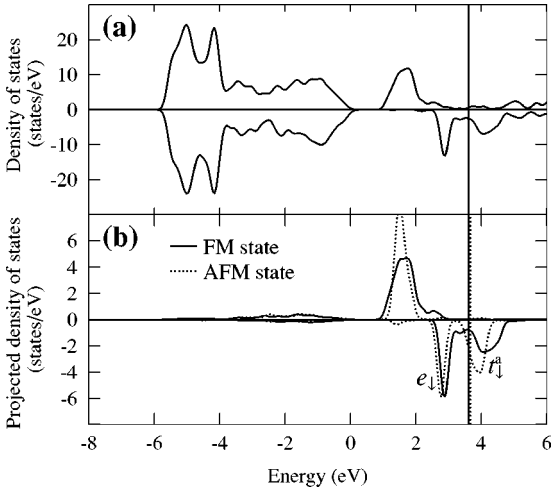

FIG. 5. For the n-type doping with an electron per Co ion, the (a) total and (b) projected densities of states onto one of the Co ions aligned along the $\boldsymbol{a}_1$ direction are drawn. The solid and dotted lines indicate the FM and AFM states, respectively, and the vertical lines denote the Fermi level. Note that the Co $3d$-derived bands are broadened due to the increase of the Co concentration by twice, as compared to that in Fig. 1.

Although spontaneous magnetization is not expected in intrinsic Co-doped ZnO, it is possible to obtain the ferromagnetic ordering in this material by electron doping. Actually, Fig. 3 illustrates that electron doping generally enhances the stability of the FM state, with an exception. In the case of continuously aligned Co ions, the FM state is greatly stabilized when electrons are doped above 0.5 electrons per Co atom. At the doping level of one electron per Co atom, the FM state is more stable by 94 and 69 meV per Co atom for the alignments along the $\boldsymbol{a}_1$- and c-axis directions, respectively. For Co pairs formed along the $\boldsymbol{a}_1$ axis, although the stability conversion from AFM to FM states occurs at a doping level higher than 0.5 electrons per Co atom, the stabilization of the FM state is significant after the doping of one electron per Co atom, while the stability of the AFM state is almost unaffected for Co pairs along the c-axis direction. When the Fermi level increases by electron doping, doped electrons occupy both the conduction band and the t^a state of minority spins [see Fig. 5(a)]. Comparing the Co $3d$-projected densities of states for the AFM and FM states, we note that the bandwidth of the t^a band is much broadened for the FM state, as shown in Fig. 5(b), and thereby the kinetic energy is lowered. Thus, the important mechanism for stabilizing the FM state is likely to be double exchange

interactions induced by carriers, which were originally proposed by Zener.[20] We check the change of magnetic interactions after electron doping for the Co-Co distances larger than 4 Å. As shown in Table I, we find no noticeable change in the magnetic state, which suggests that the range of FM interactions is also short, similar to that for AFM interactions. In addition, our calculations indicate that FM interactions weakly depend on the direction of aligned Co ions as well as the Co-Co distance. The Co-Co distances along the $\boldsymbol{a}_1$- and c-axis directions slightly differ by 0.05 Å in the wurtzite structure used here; however, different magnetic interactions along these two axes do not originate from such a small difference in the Co-Co distance. Even if we use the ideal c/a ratio of $\sqrt{8/3}$, which makes the same Co-Co distances, we find that the results remain unchanged. Thus, the use of the RKKY model,[12] which has long-range interactions with no directional dependence, may be inappropriate for Co-doped ZnO.

Based on our results, we suggest optimum experimental conditions for obtaining ferromagnetism in Co-doped ZnO. As discussed above, the first requirement is to increase the number of itinerant d electrons, which is sufficient enough for the FM coupling to prevail against the AFM superexchange interaction. This suggestion can explain the ferromagnetic ordering observed in samples with very high electron carrier densities of about 10^{20} cm^{-3}.[3] However, we point out that electron doping does not always guarantee the occurrence of ferromagnetic ordering; for Co-Co distances larger than 4 Å, the electron doping affects the magnetic coupling little. In fact, some experiments failed in obtaining ferromagnetic samples even with high carrier densities over 10^{20} cm^{-3}.[10] Thus, as a second requirement that ensures for the ferromagnetic ordering, we suggest that a large amount of Co ions should be incorporated to reduce the Co-Co distance and thus meet the short-range characteristics of ferromagnetic interactions. For a given Co concentration, a clustering of Co_{Zn} ions may enhance the stability of the FM state, as compared to a uniformly distributed configuration. However, it is a very difficult task to satisfy both the conditions in sample preparation. As the amount of incorporated Co ions increases, the number of doped electrons per Co may decrease due to the solubility limit of donor impurities, making it difficult to fulfill the first requirement. For example, concentrations of single donor impurities as high as 10^{22} cm^{-3} are needed to achieve the doping level of one electron per Co ion in $Zn_{0.75}Co_{0.25}O$, which is practically unachievable in experiments. If the amount of doped electrons is not sufficient, our calculations indicate that the AFM coupling is more preferable with increasing Co density, while previous calculations suggested that the strength of FM interactions is proportional to the Co density.[11] Experimentally, the ferromagnetic ordering was actually found in $Zn_{0.95}Co_{0.05}O$ and $Zn_{0.85}Co_{0.15}O$ but not in $Zn_{0.75}Co_{0.25}O$,[3] consistent with our results. The reason for the low reproducibility of ferromagnetic samples seems to be due to the competing aspect of the two conditions. Finally, our results also possibly explain the low saturation magnetization per Co ion observed by experiments.[21] If the two conditions are locally fulfilled in samples, the ferromagnetic ordering may appear in limited local areas, while most areas are in a spin-glass-like state, resulting in a weak spontaneous magnetization. In this case, however, we do not exclude the possibility that small magnetic moments are due to Co-metal clustering or other secondary phases.

In conclusion, we have investigated the nature of magnetic interactions between Co ions in ZnO through first-principles spin-density functional calculations. Due to antiferromagnetic superexchange interactions between Co ions, Co-doped ZnO prefers to the spin-glass-like state, while the ferromagnetic state is stabilized by electron carriers. We find that the ferromagnetic coupling has a short range nature, effective at Co-Co distances of about 3 Å, and suggest that very high concentrations of Co ions are needed to achieve ferromagnetism, with electron carriers sufficient enough to induce the ferromagnetic interaction.

This work was supported by the MOST of Korea through the National Science and Technology Program (Grant No. M1-0213-04-0001). Calculations were done using the PWSCF package.[22]

[1] H. Ohno, Science **281**, 951 (1998).
[2] Y. Ohno, D.K. Young, B. Beschoten, F. Matsukura, H. Ohno, and D.D. Awschalom, Nature (London) **402**, 790 (1999).
[3] K. Ueda, H. Tabata, and T. Kawai, Appl. Phys. Lett. **79**, 988 (2001).
[4] M.L. Read, N.A. El-Masry, H.H. Stadelmaier, M.K. Ritums, M.J. Reed, C.A. Parker, J.C. Roberts, and S.M. Bedair, Appl. Phys. Lett. **79**, 3473 (2001).
[5] S. Cho, S. Choi, G.-B. Cha, S.C. Hong, Y. Kim, Y.-J. Zhao, A.J. Freeman, J.B. Ketterson, B.J. Kim, Y.C. Kim, and B.-C. Choi, Phys. Rev. Lett. **88**, 257203 (2002).
[6] M. Rebien, W. Henrion, M. Bär, and Ch.-H. Fischer, Appl. Phys. Lett. **80**, 3518 (2002), and the references therein.
[7] H.-J. Lee, S.-Y. Jeong, C.R. Cho, and C.H. Park, Appl. Phys. Lett. **81**, 4020 (2002).
[8] S.G. Yang, A.B. Pakhomov, S.T. Hung, and C.Y. Wong, IEEE Trans. Magn. **38**, 2877 (2002).
[9] Y.M. Cho, W.K. Choo, H. Kim, D. Kim, and Y. Ihm, Appl. Phys. Lett. **80**, 3358 (2002).
[10] Z. Jin *et al.*, Appl. Phys. Lett. **78**, 3824 (2001).
[11] K. Sato and H. Katayama-Yoshida, Jpn. J. Appl. Phys., Part 2 **39**, L555 (2000); Phys. Status Solidi B **229**, 673 (2002).
[12] A.F. Jalbout, H. Chen, and S.L. Whittenburg, Appl. Phys. Lett. **81**, 2217 (2002).
[13] J.H. Kim, J.B. Lee, H. Kim, D. Kim, Y. Ihm, and W.K. Choo, IEEE Trans. Magn. **38**, 2880 (2002).
[14] J.P. Perdew, in *Electronic Structure of Solids*, edited by P. Ziesche and H. Eschrig (Akademie-Verlag, Berlin, 1991).
[15] D. Vanderbilt, Phys. Rev. B **41**, 7892 (1990).
[16] Exceptionally, our k points used for the $3\times2\times1$ supercell are

equivalent to those generated by the $9\times8\times4$ Monkhorst-Pack mesh for the $1\times1\times1$ cell.

[17] J.B. Goodenough, *Magnetism and the Chemical Bond* (Interscience, New York, 1963).

[18] P.W. Anderson, Phys. Rev. **115**, 2 (1959).

[19] Y.-J. Zhao, T. Shishidou, and A.J. Freeman, Phys. Rev. Lett. **90**, 047204 (2003).

[20] C. Zener, Phys. Rev. **82**, 403 (1951).

[21] Using experimental data in Refs. 7–9, we estimate the magnetic moments ranging from $0.01\mu_B$ to $0.26\mu_B$ per Co atom. In some cases, our estimates are different from those claimed in the references.

[22] S. Baroni, A. Dal Corso, D. de Gironcoli, and P. Giannozzi, http://www.pwscf.org.

[23] Here we choose the lattice vectors $\boldsymbol{a}_1$ and $\boldsymbol{a}_2$, with an angle of 60° between these two vectors.